

Method for Analyte Identification Using Isotachopheresis and a Fluorescent Carrier Ampholyte Assay

M. Bercovici,[†] G. V. Kaigala,[‡] and J. G. Santiago^{*,‡}

Departments of Aeronautics and Astronautics and Mechanical Engineering, Stanford University, Stanford California 94305

We present a novel method for identification of unlabeled analytes using fluorescent carrier ampholytes and isotachopheresis (ITP). The method is based on previous work where we showed that the ITP displacement of carrier ampholytes can be used for detection of unlabeled (non-fluorescent) analytes. We here propose a signal analysis method based on integration of the associated fluorescent signal. We define a normalized signal integral which is equivalent to an accurate measure of the amount of carrier ampholytes which are focused between the leading electrolyte and the analyte. We show that this parameter can be related directly to analyte effective mobility. Using several well characterized analytes, we construct calibration curves relating effective mobility and carrier ampholyte displacement at two different leading electrolyte (LE) buffers. On the basis of these calibration curves, we demonstrate the extraction of fully ionized mobility and dissociation constant of 2-nitrophenol and 2,4,6-trichlorophenol from ITP experiments with fluorescent carrier ampholytes. This extraction is based on no a priori assumptions or knowledge of these two toxic chemicals. This technique allows simultaneous identification of multiple analytes by their physicochemical properties in a few minutes and with no sample preparation.

Isotachopheresis (ITP) is used frequently in separation and detection of analytes in a wide range of applications from pharmacology and genetics to toxin detection and food analysis.^{1,2} ITP detection can be accomplished by measuring changes in conductivity, in UV absorbance, or in fluorescence intensity. Identification is typically the process of determining the identity of one or more analytes which caused an observed change in signal. This process can be difficult when there are multiple analytes of interest whose properties are not known a priori. For such applications, identification must rely on a more general approach of characterizing physicochemical properties such as mass, charge, dissociation constant, or electrophoretic mobility.

Hirokawa and Kiso³ and later Jokl et al.⁴ and Pospichal et al.⁵ used multiple ITP experiments to characterize the fully ionized mobilities and dissociation constants of a large number of ionic species. They measured the conductivity of a zone at several pH values and used a computer simulation to determine the mobility and pK_a values which best fit the data. Recently, Chambers and Santiago⁶ suggested that a similar approach can be employed for the identification of analytes from indirect fluorescence-based detection. In this work, we demonstrate how a fluorescent carrier ampholytes assay we recently developed⁷ can be used to both identify and quantitate analyte ions with little or no a priori information regarding their mobility or their acid or base dissociation constants.

We previously presented⁸ a new method for indirect detection of analytes based on ITP and fluorescent carrier ampholytes (FCA). The method requires very little or no sample preparation steps. For the FCA assay, we prepare a mixture of fluorescently tagged carrier ampholytes in a trailing electrolyte⁷ (TE) for ITP. In the absence of analytes, the tagged CAs focus at the interface between the leading electrolyte (LE) and TE and create a contiguous, baseline fluorescent zone. When analytes are present and also focus at the interface, they displace groups of CAs and create gaps in the signal. Figure 1 schematically depicts this process. In analysis of the signal, each gap in the signal denotes the existence of an analyte and the width of the gap is directly proportional to the initial concentration of the analyte.⁹ In application of this technique, one would first study the ampholyte signals in the presence of a control matrix (e.g., tap water) to establish a baseline signature associated with its ionic content. Once a baseline is established, the detection of unknown analytes would be achieved by registering their modulation with this baseline fluorescence signal. We further discuss related details of this indirect detection assay elsewhere.⁷

We here demonstrate how signals from this FCA assay can be analyzed to achieve quantitative identification of analyte ions given little or no a priori knowledge regarding their physicochem-

* To whom correspondence should be addressed. 440 Escondido Mall, Bldg. 530, Room 225, Stanford, California 94305. E-mail: juan.santiago@stanford.edu. Fax: (650) 723-7657.

[†] Department of Aeronautics and Astronautics.

[‡] Department of Mechanical Engineering.

(1) Auroux, P.; Iossifidis, D.; Reyes, D. R.; Manz, A. *Anal. Chem.* **2002**, *74*, 2637–2652.

(2) Dittrich, P. S.; Tachikawa, K.; Manz, A. *Anal. Chem.* **2006**, *78*, 3887–3908.

(3) Hirokawa, T.; Kiso, Y. *J. Chromatogr., A* **1982**, *252*, 33–48.

(4) Jokl, V.; Polásek, M.; Pospichalová, J. *J. Chromatogr., A* **1987**, *391*, 427–432.

(5) Pospichal, J.; Gebauer, P.; Bocek, P. *Chem. Rev.* **1989**, *89*, 419–430.

(6) Chambers, R. D.; Santiago, J. G. *Anal. Chem.* **2009**, *81*, 3022–3028.

(7) Bercovici, M.; Kaigala, G. V.; Backhouse, C. J.; Santiago, J. G. *Anal. Chem.* **2009**, DOI: 10.1021/ac902526g.

(8) Kaigala, G. V.; Bercovici, M.; Behnam, M.; Elliott, D. G.; Santiago, J. G.; Backhouse, C. J. Manuscript in preparation.

(9) Khurana, T. K.; Santiago, J. G. *Anal. Chem.* **2008**, *80*, 279–286.

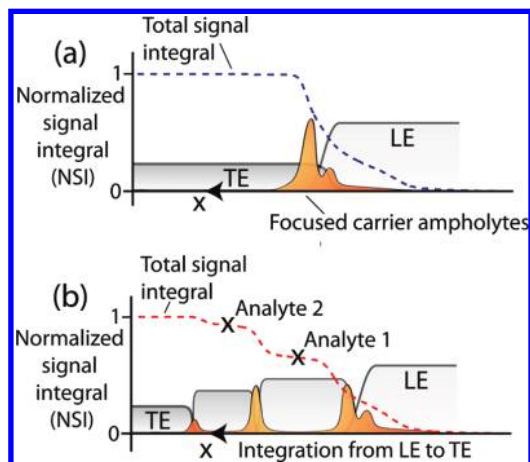


Figure 1. Schematic of isotachopheric separation and indirect detection using the FCA assay: (a) in the absence of analytes, labeled CAs focus at the LE–TE interface creating a continuous fluorescence signal and (b) analytes focused under isotachopheresis displace subsets of the labeled CAs creating gaps in the signal. The NSI (dashed curves) is a cumulative integral of the fluorescence signal from LE to TE. Plateau regions in the NSI (marked by an \times) are associated with gaps in the fluorescent signal and the presence of specific focused analytes. The NSI value for each analyte is a measure of the fraction of CA between the analyte and the LE. The latter fraction can be related to the effective analyte mobility.

ical properties. We found that the amount of displaced fluorescent CAs can be directly related to the effective mobility of the unlabeled (nonfluorescent) analyte that displace them. By constructing a calibration curve for this property, we are able to obtain quantitative measurements of the effective mobilities of analytes. Using approaches similar to that used by Hirokawa and Kiso³ and that proposed by Chambers and Santiago,⁶ we obtain an estimate of the effective mobility of analytes using two LE buffers. We then combine these measurements with ITP theory to compute estimates of the dissociation constant and fully ionized mobility of analytes. This analysis method is tailored for the FCA assay and enables rapid (~ 3 min) identification of unlabeled analytes.

We here illustrate the identification technique by applying it to two chemical pollutants: 2-nitrophenol (2NP) and 2,4,6-trichlorophenol (TCP), with no sample preparation steps. We begin by describing several principles and definitions and then show how to construct the calibration curves. We then use these curves to extract effective mobilities of detected species. Lastly, we describe how to obtain acid dissociation constants (pK_a) and fully ionized mobility values from those effective mobilities.

PRINCIPLE AND DEFINITIONS

Figure 1 presents a schematic of the FCA assay. We define an axial coordinate, x , pointing from LE to TE. In the control ITP run, labeled carrier ampholytes are focused between the LE and TE creating a continuous (albeit nonuniform) fluorescence signal. The dashed line in Figure 1a shows the cumulative integral of the fluorescent signal along x . The initial value of the integral is set to zero in the LE region where no labeled CAs are present. The integral increases monotonically until reaching a constant at the TE (where again no labeled CAs are present). For a given CA mixture and LE and TE buffer combination, this total signal integral is fixed and represents the cumulative intensity of all labeled CAs which focus at these conditions. We then define the

quantity *NSI* (for “normalized signal integral”) as the local integral value divided by the total integral,

$$NSI(x) = \int_{x_{LE}}^x [I(x) - I(x_{LE})] dx / \left[\int_{x_{LE}}^{x_{TE}} [I(x) - I(x_{LE})] dx \right]$$

where I is the fluorescence signal (averaged across the channel width) and x_{LE} and x_{TE} are axial coordinates in the LE and TE zones, respectively. When I is obtained using a point detector, the coordinate x should be replaced with the time coordinate t . In the latter case, the definition of NSI makes it independent of the intensity of illumination, exposure time, or background signal. However, data obtained from 2D images (as in this work) has to be first corrected for nonuniform illumination and background. We describe the latter process in the Supporting Information.

As shown in Figure 1b, analyte ions which focus between the LE and TE displace subsets of CAs and thus create gaps in the fluorescence signal. While the total signal integral remains unchanged (fixed total amount of CAs), the shape of the NSI function changes and now includes a new region of locally nearly constant value of NSI. This plateau corresponds to an analyte zone (where few CAs are present). The location of this analyte-specific plateau in the NSI signal is determined by the analyte’s effective mobility (see Everaerts for a description of effective versus fully ionized mobility). A species with a higher effective mobility results in a larger fraction of CAs being displaced and an associated lower NSI value for its plateau. If the exact content of the CA mixture were known (mobility and pK_a values of all species), one would be able to derive an analytical relation between the effective mobility of an analyte and its corresponding NSI. However, since the exact content of CA mixtures is unknown (typically proprietary information for the CA supplier), we construct empirical calibration curves as described in the following sections.

EXPERIMENTAL SECTION

Carrier Ampholytes Tagging. We used ZOOM 9-11 carrier ampholyte obtained from Invitrogen (Carlsbad, CA) and labeled them with Alexa Fluor 647, also from Invitrogen. The labeling protocol is similar to the one suggested by Invitrogen for labeling of proteins,¹¹ and details are provided in Bercovici et al.⁸

Materials and Instrumentation. We used two LE buffers in the experiments. LE₁ was composed of 10 mM lactic acid and 20 mM bistris (pH 6.4) in deionized water (UltraPure DNase/RNase free distilled water, GIBCO Invitrogen, Carlsbad, CA). LE₂ was identical to LE₁, with the addition of 4 mM sodium hydroxide (pH 6.8). The TE was composed of 10 mM tricine and 20 mM bistris in all experiments, but the concentration of analytes and labeled CAs (which were mixed with the TE buffer) varied between experiments and are provided in the figure captions. To both the LE and TE we added 1% ~ 1 MDa poly(vinylpyrrolidone) (PVP) for suppression of electroosmotic flow (EOF).

(10) Everaerts, F. M.; Beckers, J. L.; Verheggen, T. P. *Isotachopheresis: Theory, Instrumentation, and Applications*; Elsevier Science & Technology: Amsterdam, The Netherlands, 1976.

(11) Invitrogen MP-00143: Amine-Reactive Probes, 2007.

Table 1. List of Ionic Species and Their Properties, As Used in the Calculation of Effective Mobilities Appearing in the Calibration

species	relevant valence	fully ionized mobility [m^2/Vs]	pK_a
lactic acid (LE)	-1	36.5×10^{-9}	3.86
tricine (TE)	-1	30.0×10^{-9}	8.1
bis-tris (counterion)	+1	26.0×10^{-9}	6.4
sodium (counterion)	+1	51.9×10^{-9}	13.7
MES	-1	28.0×10^{-9}	6.1
ACES	-1	31.3×10^{-9}	6.84
MOPS	-1	26.9×10^{-9}	7.2
HEPES	-1	23.5×10^{-9}	7.5

We construct calibration curves (Figure 3) using known concentrations of very well characterized weak electrolytes. For this purpose, we used $20 \mu M$ 2-(*N*-morpholino)ethanesulfonic acid (MES), $30 \mu M$ *N*-(2-acetamido)-2-aminoethanesulfonic acid (ACES), $40 \mu M$ 3-(*N*-morpholino)propanesulfonic acid (MOPS), and $50 \mu M$ 4-(2-hydroxyethyl)-1-piperazineethanesulfonic acid (HEPES) and mixed these in the TE together with $1 \mu M$ of labeled CAs (we performed limited additional experiments where we included individual additions of these to verify their identities). We diluted these ideal analytes to their final concentration from 1 M stock solutions. For the experiments demonstrating the identification of phenols, we prepared stock solutions of 1 mM 2,4,6-trichlorophenol and 10 mM 2-nitrophenol. All buffers and analytes were obtained from Sigma Aldrich (St. Louis, MO).

We performed the experiments using an inverted epifluorescent microscope (IX70, Olympus, Hauppauge, NY) equipped with a 100 W mercury bulb (Ushio Inc., Tokyo, Japan), XF100-2 filtercube from Omega Optical (Brattleboro, VT), a $10\times$ (NA = 0.3) UPlanFl objective and a $0.63\times$ nonparfocalizing adapter. Images were captured using a 12 bit, 1300×1030 pixel array CCD camera (Micromax1300, Princeton Instruments, Trenton NJ). We controlled the camera using Winview32 (Princeton Instruments, Trenton NJ) and processed the images with MATLAB (R2007b, Mathworks, Natick, MA). We applied voltage using a high-voltage sourcemeter (model 2410, Keithley Instruments, Cleveland, OH). We used off-the-shelf microfluidic borosilicate chips (model NS-95) from Caliper Life Sciences (Mountain View, CA). The channel is isotropically etched with a depth of $12 \mu m$ and consists of a $54 \mu m$ wide section which constricts into a $34 \mu m$ wide section. The total length of the channel is 34.6 mm, with the initial (wide) section 11.5 mm in length. All images shown here were captured in the narrow region of the channel at a distance of 18.5 mm from the TE reservoir, 7 mm from the constriction.

RESULTS AND DISCUSSION

Construction of a Calibration Curve. We first present the technique for construction of calibration curves. These curves relate NSI values to effective mobility. In this example we use LE_2 and perform an FCA experiment to detect simultaneously the well characterized analytes listed earlier. A list of the analytes, their dissociation constants, and fully ionized mobilities are provided in Table 1. Parts a and b of Figure 2, respectively, present the control signal (in the absence of analytes) and the detection signal, showing four new gaps in the signal, corresponding to the focused analytes. Despite their relatively high

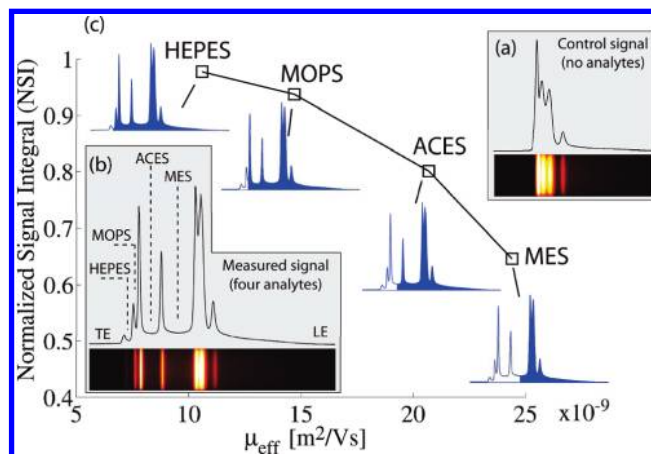


Figure 2. Construction of a calibration curve relating the value of NSI (area under the fluorescence signal) to the effective mobility of the analyte. (a) The control FCA signal in the absence of analytes (raw images of FCA signal shown with the vertical dimension magnified 25-fold for clarity of presentation). (b) FCA signal for the case with four idealized, calibrant analytes ($20 \mu M$ MES, $30 \mu M$ ACES, $40 \mu M$ MOPS, and $50 \mu M$ HEPES) with known electrophoretic mobility and pK_a values. The assay was used for indirect detection of the analytes wherein groups of FCAs are displaced by the analytes, forming gaps (or “valleys”) in the fluorescent signal (again, raw image data shown). (c) We calculate NSI values specific to each calibrant analyte using the integral of the FCA signal from LE to each analyte plateau. We plot this value versus the computed effective mobilities of the calibrants. This monotonic curve is used to extract the effective mobilities of unknown analytes given measurements of their NSI.

concentrations, the MOPS and HEPES zones are significantly shorter than the MES and ACES zones. This is expected since the focusing rate of each analyte is proportional to the ratio of its effective mobility to the effective mobility of the TE.¹² For a given pH, weak acids with higher pK_a values have lower effective mobilities, accumulate at a lower rate, and result in shorter ITP zones.

We determine the value of the NSI for each analyte at the center of its respective plateau. The NSI can be interpreted as the area under the signal curve from the LE to the analyte. This is illustrated using the measured data (not schematics) in Figure 2c, where the NSI value corresponds to the blue region under the curve. For this calibration case of known LE and known idealized analytes, we can analytically compute the effective mobilities of each of these analytes.¹⁰ With this information, we construct Figure 2c, which shows the monotonic curve relating analyte NSI value with its (here) known effective mobility.

With the use of this curve (and/or fits to this curve), NSI measurements of unknown analytes can be related to effective mobility values. The accuracy clearly depends on the resolution of the calibration curve. Lastly, we repeat this process and construct a second calibration curve for the same CAs and ideally analyze but now using LE_1 .

Extraction of 2-Nitrophenol Effective Mobilities. Parts a and b of Figure 3 present the indirect detection of 2NP using results from two different ITP buffer systems (LE_1 and LE_2). The two buffer systems are nearly identical, except that LE_2 contains an additional 4 mM of sodium hydroxide which serves as a source of counterion titrant and increases the pH throughout

(12) Khurana, T. K.; Santiago, J. G. *Anal. Chem.* **2008**, *80*, 6300–6307.

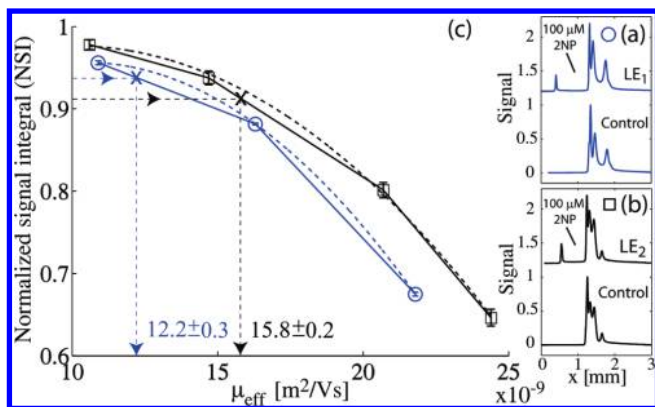


Figure 3. Extraction of the effective mobility of 2-nitrophenol (2NP) at two pH values, from two NSI calibration curves. (a) Indirect detection of 100 μM 2NP using LE₁ (pH 6.4) and (b) using LE₂ (pH 6.8). (c) We compute the NSI values of 2NP based on the two experiments and present their values as horizontal dashed lines. At the point of intersection with the appropriate calibration curve, we draw vertical dashed lines which intersect the x-axis and indicate the measured effective mobility. Solid lines correspond to linear interpolation between the data point, and the dashed curves correspond to quadratic best-fits to each of the data sets. The uncertainty bars indicate 95% confidence on the mean given three repetitions.

the ITP system. We used these experiments to compute NSI values of 2NP for the two buffers and obtained values of 0.94 and 0.91, respectively. Figure 3c presents the calibration curves for both buffer systems (the curve for LE₂ is identical to the one presented in Figure 2). We fit the data points in the calibration curves using two approximations: a linear interpolation (solid lines) and a quadratic best fit (dashed curves). In the subsequent analysis steps, we use both fitting approaches and compare their results.

We found the intersect of each NSI value with the respective curve (one intersect for each LE as shown by the horizontal dashed lines) and extract the corresponding effective mobility estimates (vertical dashed lines). Using the linear interpolation approximation, we obtain for 2NP effective mobilities of $12.2(\pm 0.3) \times 10^{-9}$ and $15.8(\pm 0.2) \times 10^{-9}$ $\text{m}^2/\text{V s}$ for LE₁ and LE₂, respectively. The uncertainty bars indicate 95% confidence on the mean given three repetitions. Using the quadratic best-fit, we obtain respective mobilities of $13.4(\pm 0.3) \times 10^{-9}$ and $16.3(\pm 0.2) \times 10^{-9}$ $\text{m}^2/\text{V s}$.

Calculation of pK_a and Fully Ionized Mobility from Effective Mobilities. Given an LE buffer composition, the properties (e.g., concentration, effective mobility, conductivity) of any ITP plateau zone can be semianalytically computed based on its fully ionized mobility and dissociation constants.¹⁰ Hirokawa and Kiso³ and later Jokl et al.⁴ and Pospichal et al.⁵ developed an iterative inverse-problem algorithm which, given a set of effective mobility measurements, computes the fully ionized mobilities and dissociation constants of the analyte. We here use the same approach but provide a graphical representation of this inverse problem, as suggested by Chambers and Santiago.⁶

Figure 4 presents two sets of effective mobility contours (dashed and solid curves), one for each LE composition. It assumes monovalent acids with pK_a values ranging from 5 to 8 and fully ionized mobilities from 15×10^{-9} to 40×10^{-9} $\text{m}^2/\text{V s}$. For each mobility versus pK_a combination (representing the properties of an individual analyte), we compute its effective

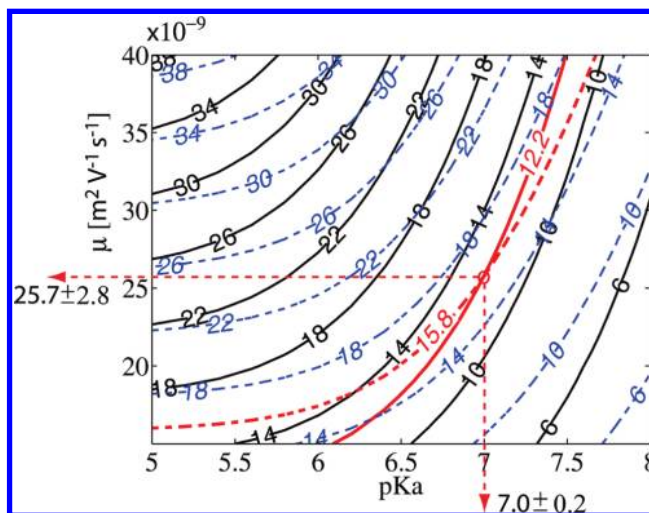


Figure 4. Extraction of fully ionized mobility and pK_a from two effective mobility measurements at two LE compositions. Two families of lines are presented, corresponding to the two compositions: LE₁ (pH 6.4, solid lines) and LE₂ (pH 6.8, dashed lines). Within each family, the contours represent the effective mobility of an analyte given the respective values of pK_a and fully ionized mobility. The intersection of two effective mobility contours (one from each family) identifies the pK_a and fully ionized mobility of a single species exhibiting these effective mobilities under the two chemistries. The thick lines indicate the effective mobility values obtained for 2NP from the fluorescent carrier ampholytes assay using the linear interpolation approximation for the calibration curves. The pK_a and fully ionized mobility of 2NP were found to be $7.0(\pm 0.2)$ and $25.7(\pm 2.8) \times 10^{-9}$ $\text{m}^2/\text{V s}$, respectively.

mobility when in a pure ITP zone. This results in contours of effective mobility values in the field of pK_a versus (fully ionized) mobility. This contour map is determined completely by the composition of the LE (e.g., does not depend on the CA or specific analytes of interest).

To obtain the fully ionized mobility and pK_a given two effective mobilities, we look for the intersection point of the contour curves corresponding to those effective mobilities. For example, for 2NP using the linear interpolation approximation, we found the nominal effective mobility to be 12.2×10^{-9} $\text{m}^2/\text{V s}$ for the system with LE₁. This places the solution along the 12.2×10^{-9} curve (marked as a thick solid line) of the LE₁ contour map. At the same time, the solution also lies on the 15.8×10^{-9} curve (marked as a thick dashed line) of the LE₂ contour map. The solution must therefore lie at the intersection point, giving a pK_a of $7.0(\pm 0.2)$ and a fully ionized mobility of $25.7(\pm 2.8) \times 10^{-9}$ $\text{m}^2/\text{V s}$. Similarly, using the quadratic best-fit approximation, we obtain a pK_a of $6.7(\pm 0.2)$ and a fully ionized mobility of $22.3(\pm 2.3) \times 10^{-9}$. We know of no previous measurements of the mobility of 2NP, but its reported pK_a value of 7.22^{13} is in good agreement with our measurement of $7.0(\pm 0.2)$.

We performed the same process using TCP and obtained respective effective mobilities of $14.4\text{--}14.7 \times 10^{-9}$ and $16.2\text{--}16.8 \times 10^{-9}$ $\text{m}^2/\text{V s}$ for LE₁ and LE₂, respectively using the linear interpolation approximation. Using the quadratic approximation, we obtained respective effective mobilities of $15.1\text{--}15.4 \times 10^{-9}$ and $16.8\text{--}17.4 \times 10^{-9}$. Here the ranges indicate the values given two repetitions of each experiment. With the use of the average

(13) Dean, J. A. *Lange's Handbook of Chemistry*, 15th ed.; McGraw-Hill: New York, 1999.

of these values, Figure 4 yields a pK_a of 6.26 and a fully ionized mobility of $19.4 \times 10^{-9} \text{ m}^2/\text{V s}$ (not shown in the figure) using the linear interpolation approximation, and a pK_a of 6.1 and fully ionized mobility of 19.5×10^{-9} using the quadratic approximation. Reported values for the pK_a of TCP range from 6.0¹⁴ to 6.23,¹⁵ again in fairly good agreement with our measurement. We note that as demonstrated by the calibration curves, multiplexed detection and identification of analytes is also possible. In the Supporting Information we present an example experiment where we detect 2NP and TCP simultaneously in the same ITP separation.

CONCLUSIONS AND RECOMMENDATIONS

We demonstrated that our fluorescent carrier ampholyte technique can be used to estimate the fully ionized mobility and dissociation constant of detected analyte ions. These physicochemical properties can be used to identify analytes with little or no a priori knowledge, short analysis time, and no sample preparation.

We have shown that the fraction of fluorescent carrier ampholytes displaced by ITP focused analytes can be quantified by integration and appropriate normalization of the fluorescence signal. To this end, we defined and presented a method for calculating a normalized value, NSI, defined as the signal integral from LE to analyte normalized by the total signal integral (from LE to TE). NSI is proportional to the amount of CA focused between the LE and analyte. We showed that the NSI of an ionic analyte is monotonic with the effective mobility it acquires in its respective ITP zone. We used this property to construct two calibration curves, based on two different LE buffers, which can be used to convert experimentally measured NSI values to effective mobility values. Once effective mobilities are obtained, we use an ITP theory (and associated effective mobility contours versus fully ionized mobility and pK_a) to retrieve the analyte ion's fully ionized mobility and pK_a . We demonstrated this process for the detection and identification of 2-nitrophenol and 2,4,6-

trichlorophenol and obtained respective dissociation constants in good agreement with published values.

In future work we will seek to improve the accuracy, resolution, and multiplexing capability of the technique. We here offer several ideas and suggestions along this line. First, additional calibrant analytes should be used to improve the accuracy of interpolation (e.g., as in Figure 3). As shown here, different approximations of the calibration curves (i.e., linear interpolation vs quadratic fit) can result in differences in extracted pK_a values of approximately 5% (e.g., pK_a 7 with linear interpolation vs pK_a 6.7 with quadratic best-fit). The results clearly depend on the resolution of the calibration curve, and we expect that additional calibration points (i.e., performing the assay on additional species whose mobility and pK_a are known) should improve the accuracy. Second, LE buffers should be selected to optimize the shape of the mobility contour map (as in Figure 4). For example, as suggested by Chambers and Santiago,⁶ LE combinations should be chosen to increase the angles between intersecting contour lines, thus minimizing the error associated with the estimates of pK_a and fully ionized mobility given inaccuracies in effective mobility measurement. Lastly, we hope to explore the practice of adding calibrant analytes to actual samples as an internal standard and simultaneous calibration in a single experiment. Further, we hope to explore the use of two simultaneous ITP runs in the same chip using a common TE reservoir, to reduce the analysis time and sample variability between runs. As we have shown in a separate work,⁸ the FCA assay can be integrated in a self-contained hand-held device. We envision implementing this identification technique and its related algorithms to enable low-cost and portable identification of analytes in point of service settings.

SUPPORTING INFORMATION AVAILABLE

Additional information as noted in text. This material is available free of charge via the Internet at <http://pubs.acs.org>.

Received for review November 10, 2009. Accepted December 26, 2009.

AC9025658

(14) *Knovel Critical Tables*, 2nd ed.; Knovel Corp.: Norwich, NY, 2003.

(15) Barták, P.; Cáp, L. *J. Chromatogr., A* **1997**, *767*, 171–175.